4D Seismic Inversion on Continuous Land Seismic Reservoir Monitoring of Thermal EOR*

Laurene Michou[1], Thierry Coleou[1], Yves Lafet[1], and Benjamin Roure[2]

Search and Discovery Article #41519 (2015)
Posted January 19, 2015

*Adapted from extended abstract prepared in conjunction with presentation at CSPG/CSEG/CWLS GeoConvention 2013, (Integration: Geoscience engineering Partnership) Calgary TELUS Convention Centre & ERCB Core Research Centre, Calgary, AB, Canada, 6-12 May 2013, Datapages/CSPG © 2015

[1]CGGVeritas, Massy, France (laurene.michou@cggveritas.com, thierry.coleou@cggveritas.com, yves.lafet@cggveritas.com)
[2]CGGVeritas, Calgary, Alberta, Canada (benjamin.roure@cggveritas.com)

Abstract

A permanent reservoir monitoring system has been installed for Shell at the end of 2010, on a medium heavy-oil onshore field situated in the northeast of The Netherlands, in the context of re-development of oil production by Gravity Assisted Steam Flood. The first challenge was to continuously monitor, with seismic reflection, the lateral and vertical expansion of the steam chest injected in the reservoir during production over more than a year. As the 4D seismic attributes obtained from monitoring fit the measurements made at observation, production and injector wells, the 2D monitoring system was extended to 3D in April 2012. The second challenge was quantify seismic amplitude variations in terms of petro-acoustic parameters. For that purpose, 4D inversion was performed on continuous 2D and 3D seismic monitoring data in order to quantify the lateral and vertical expansion of the steam chest on a daily basis. The 4D inversion results not only point out that the inversion enables to quantify the 4D effects in terms of P-impedance variations, but also greatly improves the vertical location of these events. Moreover, the percentage of maximum impedance variations and the thickness where these variations are observed are in good agreement with the petro-elastic model.

Introduction

Since December 2010, a 2D permanent seismic monitoring system has been deployed for Shell on an existing heavy oil field in Schoonebeek, The Netherlands. The aim was to evaluate its suitability for continuous seismic monitoring as a tool to optimize field development of oil production by Gravity Assisted Steam Flood. The system consists of 12 piezoelectric mini-vibrator sources cemented into dedicated boreholes at a depth of 25 meters and a set of three lines of 69 dual buried hydrophones at six and nine meters depth. The source and receiver lines are located such that they are right above the point where the two observation wells intersect the reservoir. Hornman et al. (2012) and Cotton et al. (2012) showed that quantitative time shifts and qualitative amplitude variations, calculated by cross-correlation on the seismic data, fit with the observation, production and injector well data.

As these first results were conclusive, in April 2012 the 2D monitoring system was extended to 3D (five lines of 69 dual buried hydrophones and 36 sources). Figure 1 illustrates the 2D and 3D acquisition designs and the monitoring project scheduling. In order to quantify the time-

lapse amplitude variations in terms of impedance variations, a 4D acoustic seismic inversion was performed. This paper presents the results of the 4D inversion carried on both the 2D and 3D monitoring data.

4D Inversion Methodology

The multi-vintage, global inversion starts from an initial layered model constructed using a stratigraphic grid framework defined in the time domain. In the vertical direction, grid cell thicknesses are linked with the seismic resolution, typically between two and six ms. Laterally, grid cell dimensions are fixed by the seismic trace spacing. The structure of the grid is the same for each survey time. The 4D inversion methodology is a global time-lapse inversion scheme, involving joint inversion of base and monitor data, as described by Lafet et al. (2009). All vintages and input angle stacks are combined in a single objective function, which is optimized using simulated annealing to estimate the time-variant distribution of elastic attributes that best matches all available data. The multi-vintage nature of the optimization allows us to incorporate flexible, user-defined rock physics constraints on the evolution of Vp, Vs and density between consecutive surveys. These user-defined bounds are both space and time variant, and are specified as 4D cubes of min and max values for each inverted attribute. The coupling reduces the inversion non-uniqueness and identifies solutions that are consistent with basic rock physics information. There are no restrictions on the number of input angle stacks or number of monitor surveys. This allows us to invert simultaneously hundreds of surveys.

The 4D inversion is performed in a stratigraphic grid, which provides a natural framework to handle time shifts. Between consecutive vintages, we can link the time-lapse change of Vp (ΔVp) and the time-thickness change (Δt) of each cell and thus derive monitor time from the ΔVp Base/Monitor ratio without the need to re-align seismic vintages using pre-computed time shifts. Each vintage has a specific time axis defined by a layer position whose consistency with other vintages is ensured by the ΔVp cubes during the inversion process.

The specific monitoring system induces three main consequences on the inversion process. First, the sources in the acquisition system have limited power at low frequencies. This affects both the wavelet and the influence of the initial model in the inversion response. Figure 2 shows (a) the fit between synthetic and real data at the deviated observation well 2, (b) the estimated wavelet and (c) its frequency content. The correlation is around 0.65, which is reasonable considering that we correlate a deviated well perpendicular to a 2D line.

Secondly, the seismic acquisition fold is very low with a limited offset range at the target level: below 12 for the 3D monitoring and below 36 for the 2D monitoring (in fact, the 2D monitoring line is the sum of three acquisition lines). Consequently, the 4D inversion was restricted to the estimation of acoustic impedance Ip from the total seismic stack. Finally, 4D time shifts are estimated by cross-correlation with a 100 ms sliding window. This technique allows accurate estimation of the time shift value (0.4 ms between April and August 2011), below the reservoir but cannot detect the top and the base of the interval (10 ms) that produces these time shifts. As it was not possible to accurately align the monitor data before inversion, we used the possibility to manage the time shifts during the 4D inversion as explained previously. A first constraint was that Ip variations were allowed only in the reservoir interval or close to the top or the bottom. According to the Petro Elastic Model and the injection flow rate, constraints on the possible variations of Vp and density between consecutive vintages were added.

4D Inversion of 2D Monitoring

The seismic data of the 2D monitoring were organized as two pseudo 3D cubes. For the monitor, each daily 2D line was considered as a line of a 3D cube. Figure 3 shows the Monitor cube where days are taken as the third dimension. The Base cube was constructed by duplicating one line, which was the average over one month of acquisition preceding the injection start. In order to calibrate the wavelet amplitude and build the 4D initial base model, a 3D inversion process inverted the Base cube.

Figure 4 shows the inversion results at observation well 2. On the left panel we can compare the resolution after inversion (in red) versus the initial model (in blue). The thickness of the layers in the initial model was close to 2 ms with a bin size of 8 by 8 meters. On the right track, we observe a good match between the real and synthetic data, resulting in a low level of residuals.

Figure 5 shows the 4D inversion results at the injection well, 3 months after injection started. From left to right we find: (a) P-impedance for base (blue) and monitor (red), (b) the ratio of the monitor impedance over the base impedance, which reaches -8 %, (c) and (d) the amplitude envelope of adjacent seismic traces with the synthetic seismogram for both the base and the monitor, (e) the time shifts calculated from the Vp variations. The time shift value at the base of the reservoir is comparable to the 0.4 ms time shift estimated by cross-correlation on the seismic data with 100 ms sliding windows. Panel (f) shows the amplitude variations calculated by cross-correlation on the seismic data with 20 ms sliding window. Clearly, while estimating the same order of time shift variations, the inversion process enables to focus the 4D events at the top of the reservoir as expected.

The concertina of sections in Figure 6 shows a dissymmetric decrease of P-impedance. Eastwards from the injector well the impedance anomaly seems to reach its limit by day 240. Westwards a continuous extension is visible on mainly two areas: one at the vertical of the injector well (a1) and another one slightly at the west side (a2) without any connection with the first area. To better understand the connection between these two areas, the inversion of the 3D monitoring was performed.

4D Inversion of 3D Monitoring

The 3D monitoring images a surface of 800 by 120 meters with a bin size of 8 by 8 meters. As the monitoring survey became 3D on a daily basis, the 3D cubes to be inverted were constructed as the monthly average of the seismic data. The “pseudo base cube” corresponds to the month of April 2012, i.e. one year after the start of the steam injection. As no 4D effect was detected from the 2D monitoring at the observation well 2, it was possible to estimate the 3D wavelet at this well from the 3D migrated “pseudo base cube”, as shown in Figure 7. The comparison with Figure 2 shows clearly the improvement of the fit due to 3D acquisition, 3D processing and 3D migration.

Figure 8 illustrates volumes of P-impedance variations higher than 4% since April 2012, from June to September 2012 in the reservoir. The wells are also represented. These results indicate that from the blue injector well to the western red producer well, the steam has bypassed by the north; hence, the two areas of impedance decrease on 2D sections of Figure 6. Moreover, it seems that a “barrier” prevents the steam from propagating to the eastern side towards the other producer. These results are consistent with the pressure and temperature measurements of the two observation wells.

Conclusions

The benefits of 4D inversion on the continuous seismic monitoring are the vertical resolution (2 ms) and the quantification of 4D effects in term of P-impedance variations (-8%) which were in agreement with the Petro Elastic Model. The next steps will be the quantitative validation of the P-impedance variations through the interpretation of their evolution in terms of fluid or temperature variations and to check how they fit the observations at the wells.

Acknowledgements

The authors thank Shell and NAM for their kind permission to present this work.

References Cited

Cotton, J., E. Forgues, and J.C. Hornman, 2012, Land Seismic Reservoir Monitoring: Where is the steam going?: 82nd SEG Conference & Exhibition, Extended Abstracts, p. 667-670.

Hornman, J.C., J. Van Popta, C. Didraga, and H. Dijkerman, 2012, Continuous monitoring of Thermal EOR at Schoonebeek for Intelligent Reservoir Management: SPE Intelligent Energy International, 150215.

Lafet, Y., B. Roure, P.M. Doyen, and H. Buran, 2009, Global 4D Seismic Inversion and Time-Lapse Fluid Classification: 79th SEG Conference & Exhibition, Extended Abstracts, p. 3830-3834.

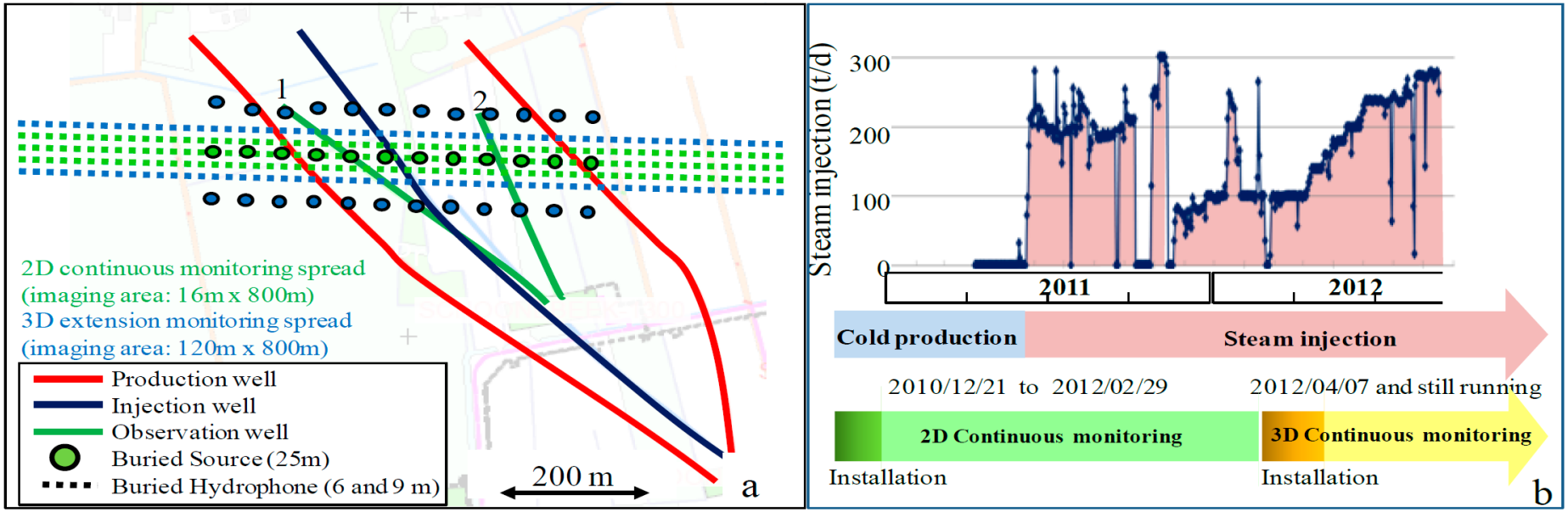

Figure 1. (a) Survey sketch map over the horizontal steam-injector/oil-producer and observation wells, (b) seismic monitoring scheduling.

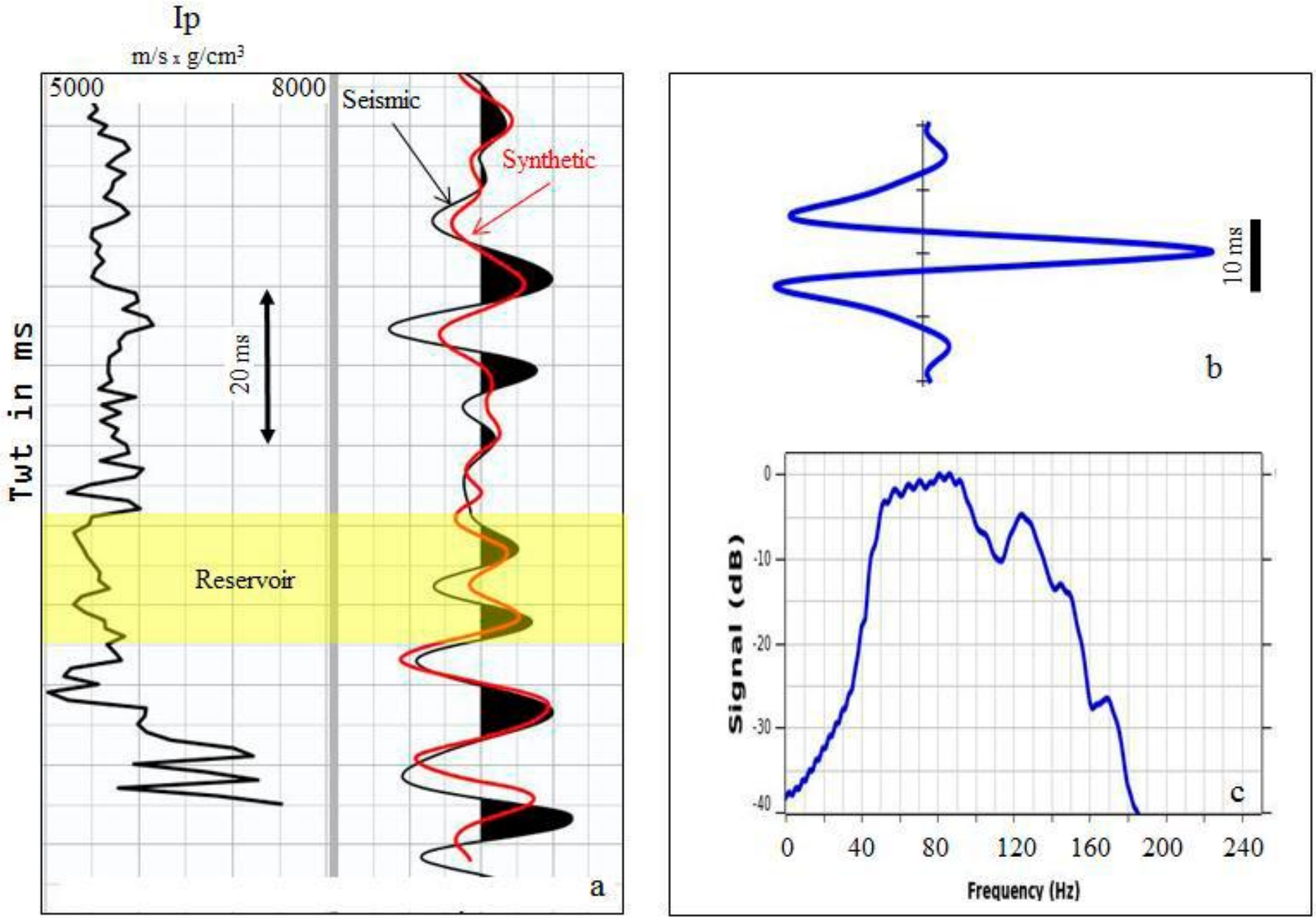

Figure 2. Wavelet estimation at deviated observation well 2: (a) 2D seismic/synthetic seismogram fit, (b) estimated wavelet, (c) amplitude spectrum.

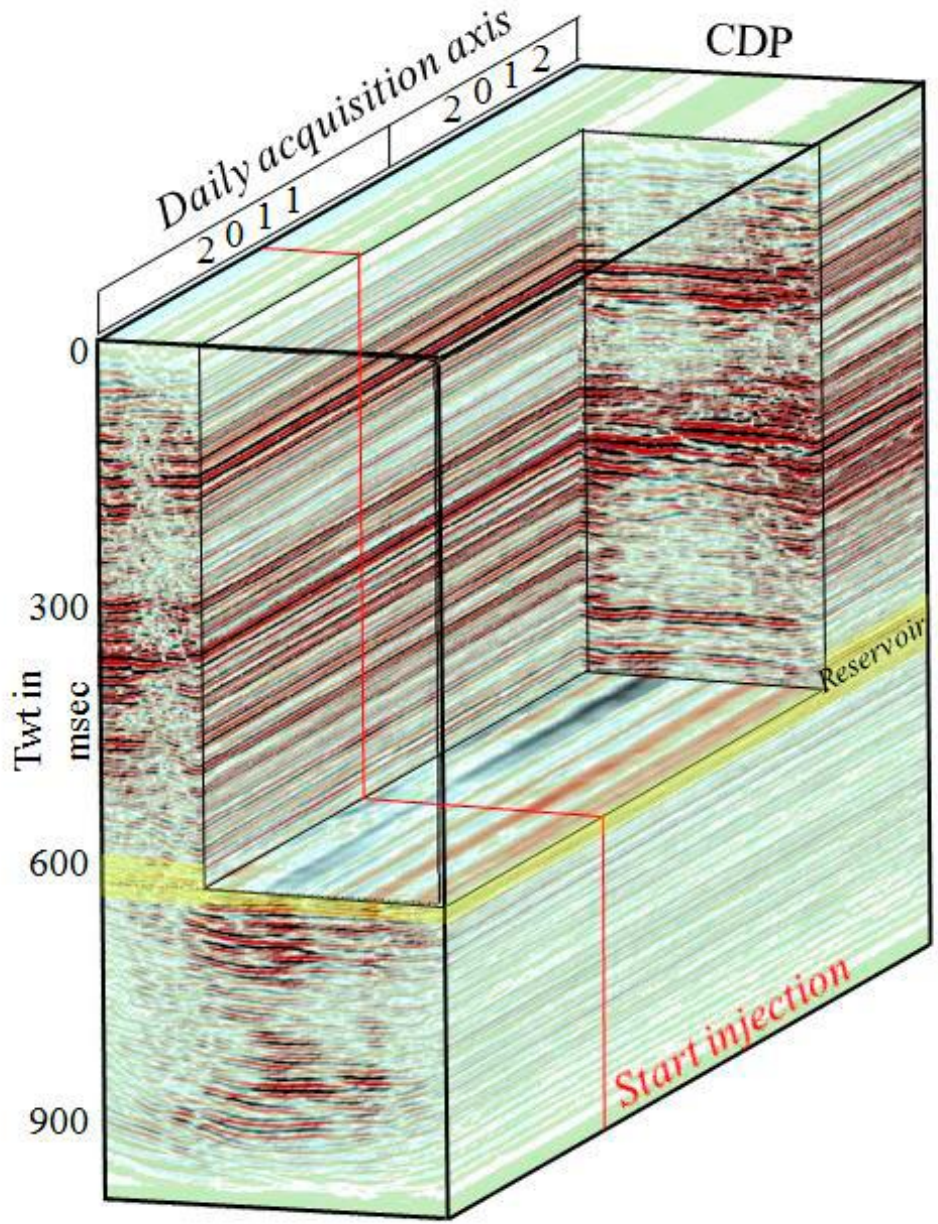

Figure 3. 2D Continuous monitoring: pseudo 3D cube.

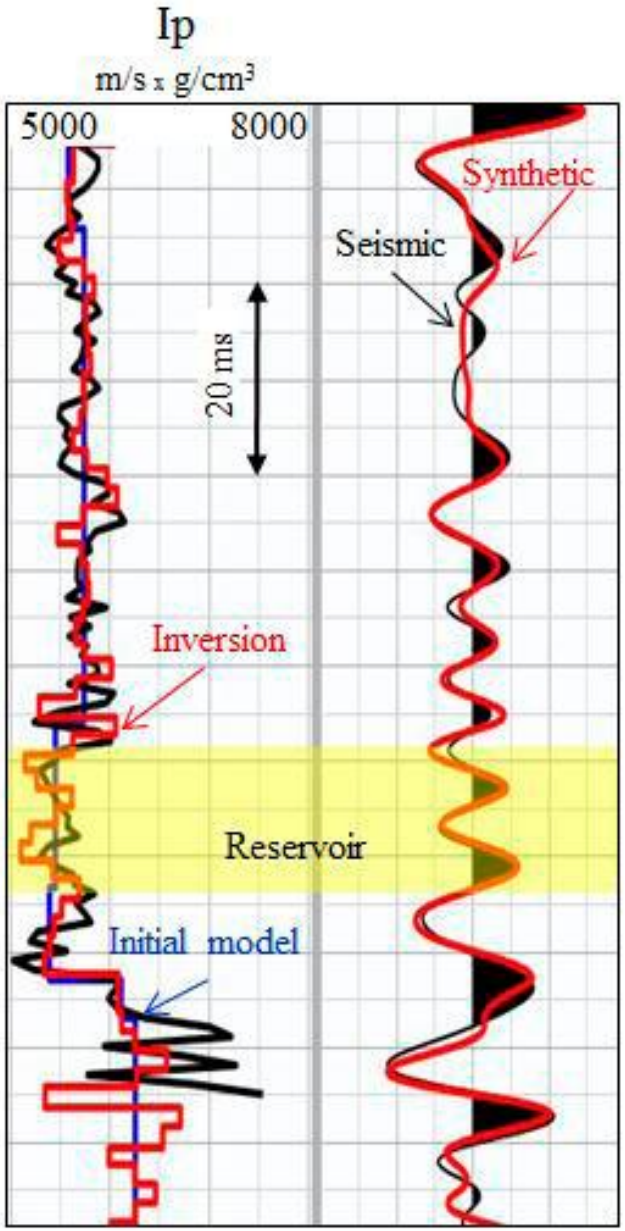

Figure 4. 3D inversion calibration at observation well 2.

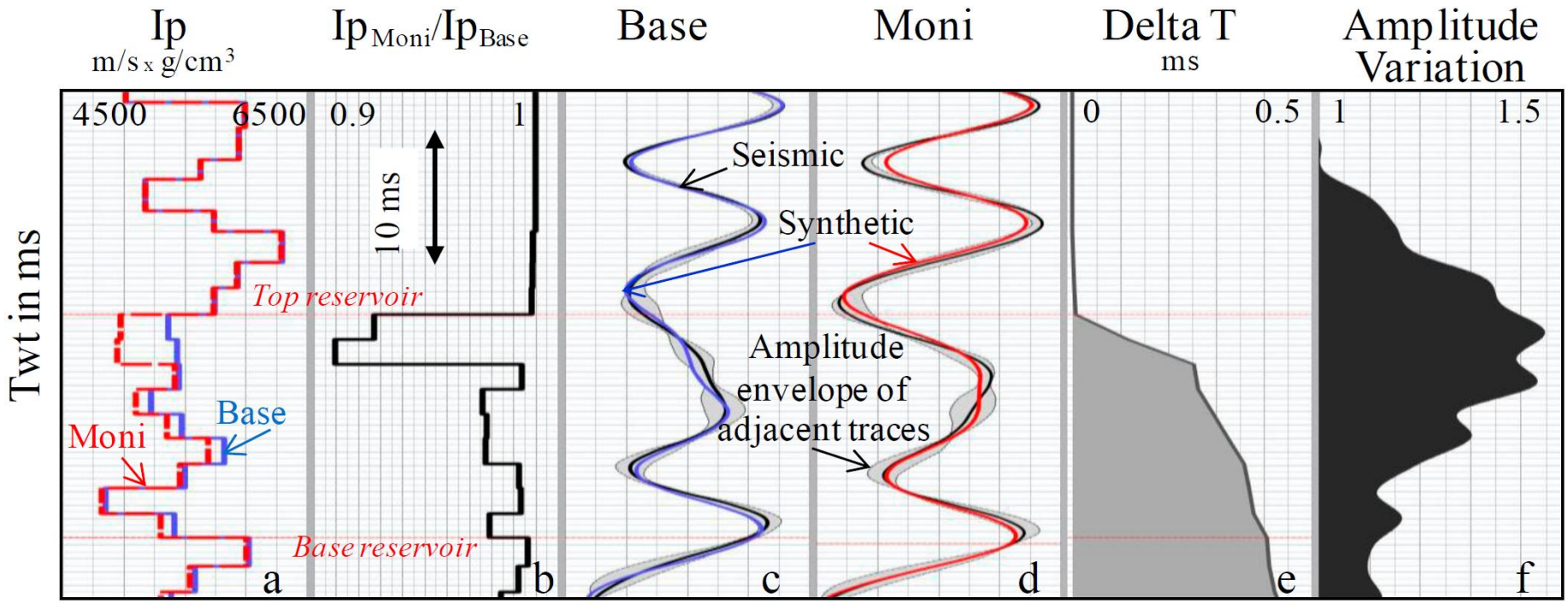

Figure 5. 4D inversion results at the injection well: (a) P-impedance for base (blue), monitor (red), (b) monitor over base impedance ratio, (c) and (d) seismic trace and synthetic seismogram for base (blue) and monitor (red), (e) time shifts from inversion, (f) base/monitor amplitude variations.

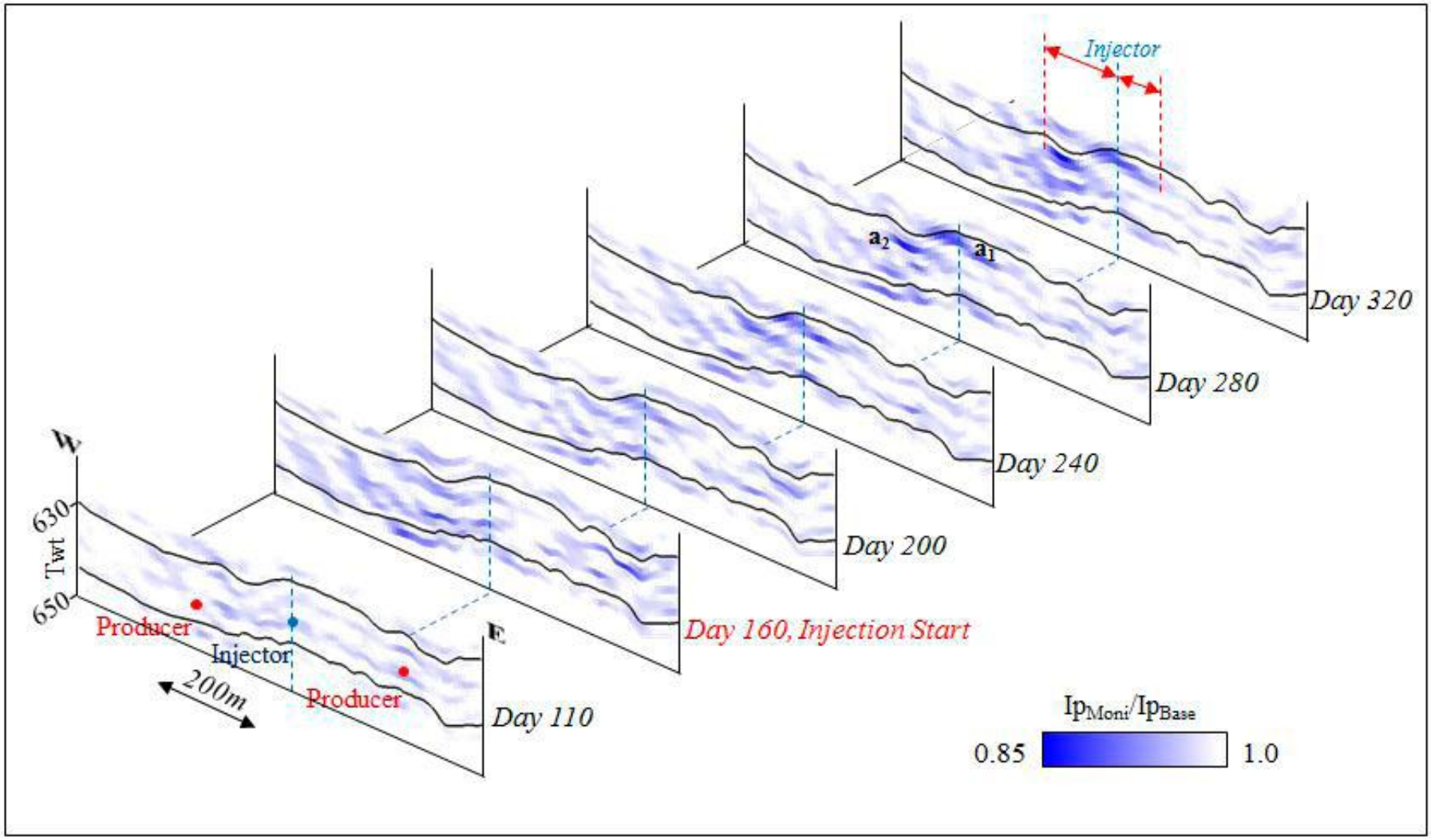

Figure 6. Successive sections of impedance variations from 2D monitoring.

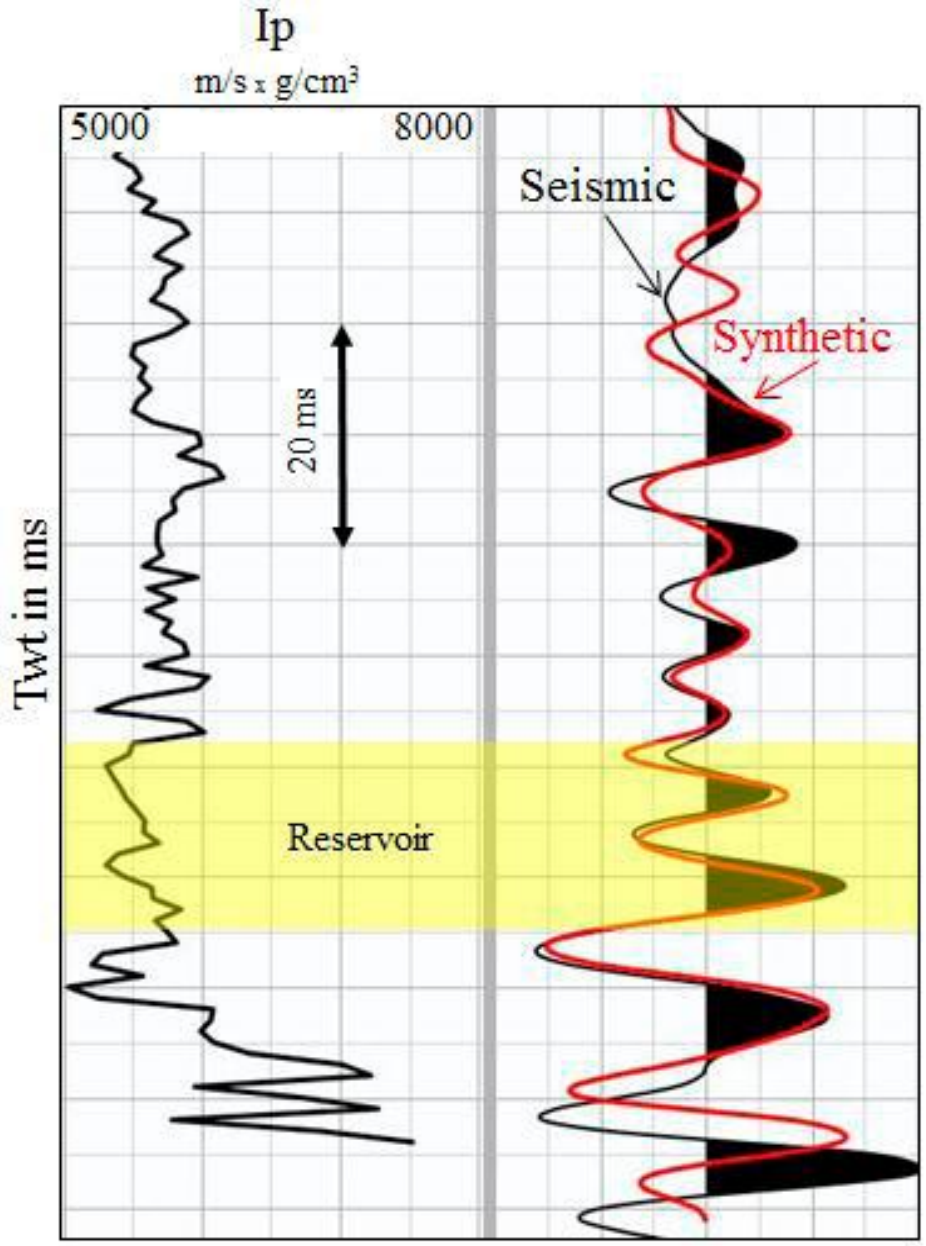

Figure 7. 3D Seismic/synthetic seismogram fit at observation well 2.

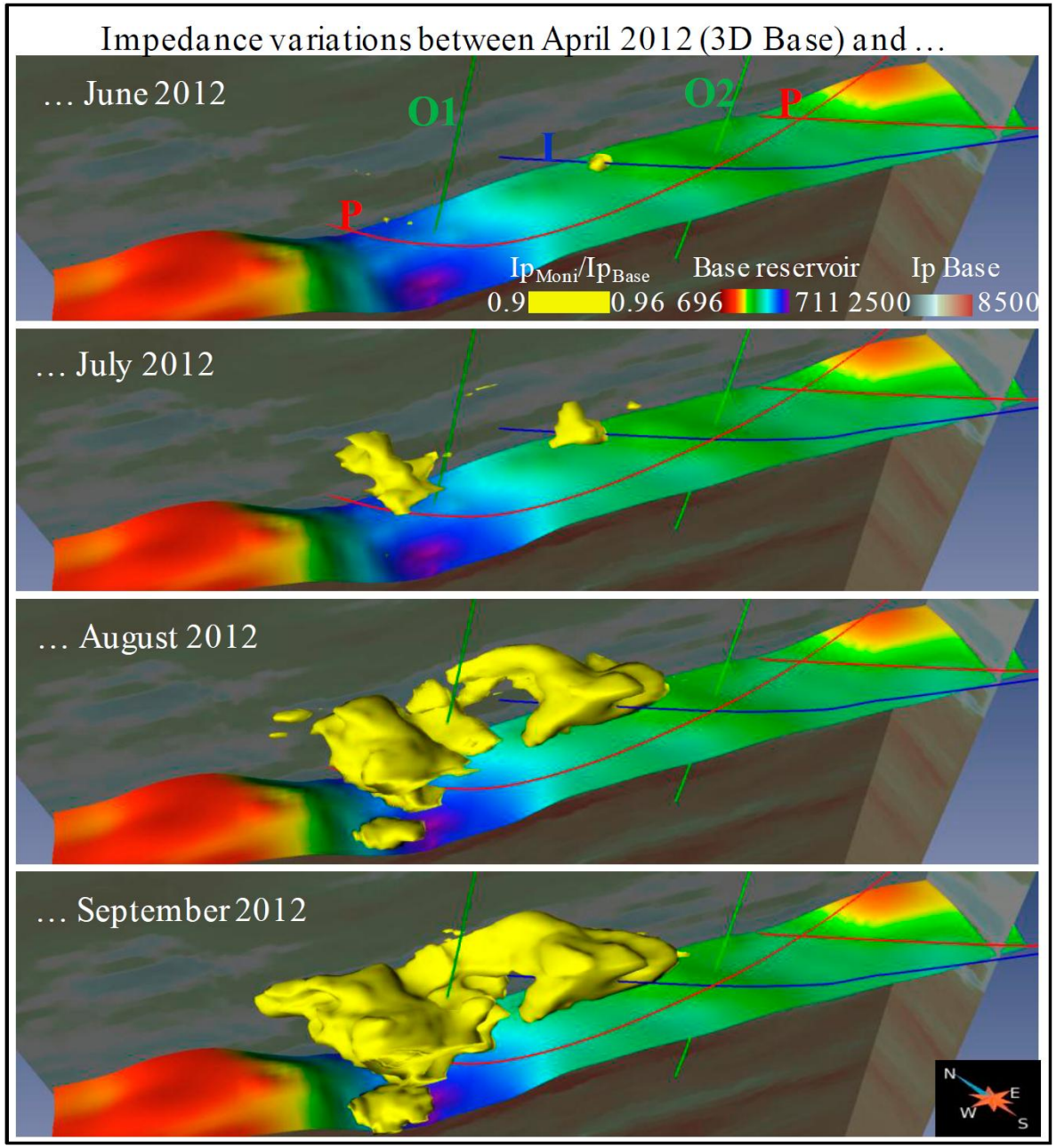

Figure 8. 3D monitoring. P impedance variations in the reservoir.